Nonlinear Dyn (2017) 88:1–19
DOI 10.1007/s11071-016-3227-x

ORIGINAL PAPER

Synchronization of uncertain fractional-order hyperchaotic systems by using a new self-evolving non-singleton type-2 fuzzy neural network and its application to secure communication

Ardashir Mohammadzadeh · Sehraneh Ghaemi

Received: 6 June 2016 / Accepted: 16 November 2016 / Published online: 2 December 2016

Abstract This paper presents a robust control method for synchronization of the uncertain fractional-order hyperchaotic systems by using a new self-evolving non-singleton type-2 fuzzy neural network (SE-NT2FNN). The proposed SE-NT2FNNs are used for estimating the unknown functions in the dynamic of system. The effects of approximation error and external disturbance are eliminated by linear matrix inequality control scheme. The proposed SE-NT2FNN has one rule initially, the new rules and membership functions (MFs) are added based on the proposed simple algorithm and unnecessary rules and MFs are deleted. The proposed synchronization scheme is applied in a secure communication scheme. To show the effectiveness of the proposed method, three simulation examples are given. The results are compared with other methods, and it showed that the proposed control scheme results in the better performance than other methods.

Keywords Self-evolving algorithm · Non-singleton type-2 fuzzy neural network · Robust LMI-based control · Fractional-order hyperchaotic

A. Mohammadzadeh · S. Ghaemi (✉)
Control Engineering Department, Faculty of Electrical and Computer Engineering, University of Tabriz, Tabriz, Iran
e-mail: ghaemi@tabrizu.ac.ir

A. Mohammadzadeh
e-mail: a.mohammadzadeh@tabrizu.ac.ir

1 Introduction

Hyperchaotic systems are high-dimensional chaotic systems with complex behavior, which have more than one positive Lyaponuv exponent. Since, these systems exhibit a behavior as noise-like, unpredictability and highly sensitive to the initial conditions, are more useful in some applications such as secure communications and encryption. Also, the fractional systems contain fractional orders, and this feature leads to more complicated chaotic behaviors which can be used in applications such as secure communications. By utilizing the fractional calculus techniques, some fractional-order chaotic/hyperchaotic systems have been identified such as fractional-order chaotic/hyperchaotic Chen system [1,2], fractional-order hyperchaotic Novel system [3] and fractional-order hyperchaos Lorenz system [4]. In [5], many systems which behave in a chaotic manner are reviewed. Also in [6–8], the some fractional discrete systems which can exhibit chaos behavior are introduced. In the chaos-based secure communication schemes, to recover the message from the transmitter, master-slave synchronization must be completely achieved. In recent years, many types of chaos synchronization approaches have been proposed, such as projective synchronization, adaptive control, robust synchronization and active pinning control [9–12].

In many practical applications, the accurate dynamics of the systems are not available or are perturbed by the external disturbances, time delays, time-varying parameters, etc. To cope with the uncertainties and

perturbations, many robust controllers have been presented. For instance in [13,14], the H_∞ control problem is investigated for the fractional-order linear systems. The mean-square exponential stability problem is studied in [15,16]. In [17], based on the matrix's singular value decomposition, some sufficient conditions for quadratic stability of the uncertain fractional-order linear systems are presented. The feedback stabilization of the fractional-order systems using linear matrix inequality technique is studied in [18,19]. The problem of the exponential synchronization of the discrete-time neural networks with mixed time delays, actuator saturation and failures, by using Lyapunov functional approach is investigated in [20]. The robust sliding mode control of the fractional-order systems is proposed in [21,22]. In [23], a robust model predictive control scheme is presented to control the fractional-order discrete-time systems.

To deal with the uncertainties in the dynamics of the system, some approaches have been presented based on the approximation property of the fuzzy neural networks (FNNs). In [24], a fuzzy sliding mode controller is proposed. A states feedback method by using LMI technique, based on fuzzy model, is proposed in [25] to stabilize the fractional-order chaotic systems. The generalized projective synchronization by estimating unknown nonlinear functions using fuzzy systems is presented in [26]. An adaptive fuzzy controller with H_∞ synchronization performance is studied in [27].

The main problem in the design of fuzzy controller is the problem of "curse of dimensionality". By increasing the input variables of a fuzzy neural network, the number of rules exponentially increases. Since the hyperchaotic systems are high-dimensional nonlinear system, FNNs cannot be adequately applied to estimate the uncertain functions in the dynamic of these systems. One approach to cope with this problem can be self-evolving FNNs.

For this purpose, some self-evolving type-2 FNNs have been proposed. For instance recently in [28], a SE-T2FNN is presented, the rule database of which is initially empty, and all rules are automatically grown. In [29], a self-evolving recurrent type-2 fuzzy radial basis function network is presented, where new neurons and rules are generated based on a clustering algorithm. In [30], a hierarchical SE-T2FNN is presented in which its new rules and antecedent part are generated by using ε-completeness criterion (this means that the firing strength of at least one fuzzy rule for any input within the operating range is not less than ε) and its consequent part is designed by using ant-colony optimization method. In [31], the rule database is modified in response to the controller's performance.

Singleton type-2 FNNs are used in all of the mentioned self-evolving algorithms, in which the linguistic and input numerical uncertainties are handled only by MFs. The input uncertainties arise from noise and inaccuracy of sensors, observers and input devises. The non-singleton type-2 FNNs are considered in [32–34]. In these papers, some learning algorithms are developed for tuning free parameters of non-singleton type-2 FNNS.

Motivated by the discussions above, in this paper, a new self-evolving non-singleton type-2 FNN is presented. The proposed self-evolving algorithm in this paper is simple, and it can be applied to the high-dimensional problems. The proposed SE-NT2FNN has only one rule initially. New MFs are added or replaced, or the existing MFs are changed such that ε- completeness criterion is satisfied. The dynamic of FOHS is assumed to be unknown and the proposed SE-NT2FNNs are employed to estimate the unknown functions. To eliminate the effect of approximation error, a LMI-based robust controller is combined with the output feedback control scheme. Some advantages of the proposed method are as follows:

- The dynamic of fractional-order chaotic system is assumed to be unknown; then the proposed controller can be applied to a wide class of FOHS.
- A new self-evolving non-singleton type-2 fuzzy neural network is presented, in which the new MFs and rules are added based on the simple algorithm, and unimportant rules are deleted. Furthermore, input uncertainties are handled by using non-singleton fuzzification.
- The effect of approximation error and external disturbance is eliminated by a proposed LMI-based robust controller.
- Since triangular type-2 MFs are employed, in each sample time, a few number of MFs are activated for each input; furthermore, interpretability of the FNN is increased.

The remaining of this paper is organized as follows. In Sect. 2, system description and problem formulation are presented. The proposed non-singleton type-2 fuzzy neural network is presented in Sect. 3. The proposed self-evolving algorithm is introduced in Sect. 4.

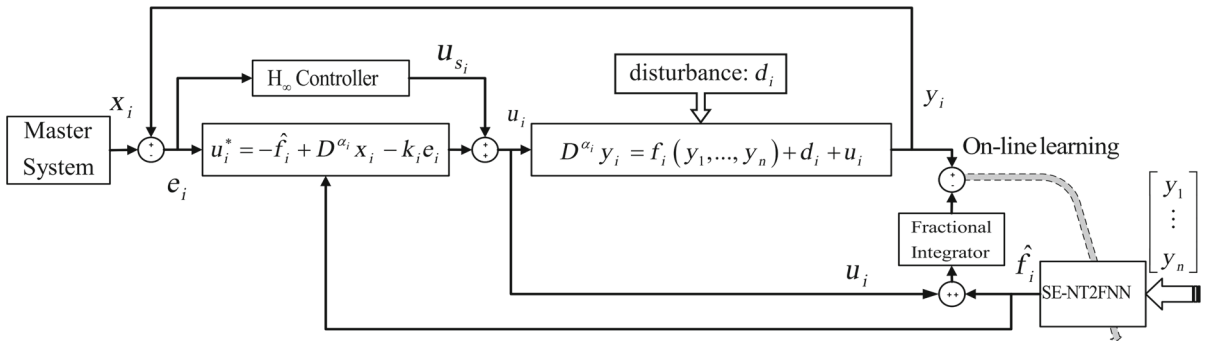

Fig. 1 Proposed control block diagram for the i-th subsystem

Stability analysis is presented in Sect. 5. The simulation results of the controlled fractional-order hyperchaotic systems are shown in Sect. 6. Finally, conclusions remarks are presented in Sect. 7.

2 Problem formulation and system description

The following class of FOHS is considered as slave system:

$$\begin{aligned} D^{\alpha_1} y_1 &= f_1(y_1, \ldots, y_n) + d_1(t) + u_1(t) \\ &\vdots \\ D^{\alpha_n} y_n &= f_n(y_1, \ldots, y_n) + d_n(t) + u_n(t) \end{aligned} \tag{1}$$

where $f_i, i = 1, 2, \ldots, n$ are unknown but bounded functions, $d_i(t), i = 1, 2, \ldots, n$ are bounded external disturbance, $u_i, i = 1, 2, \ldots, n$ are control signals, $\underline{y} = [y_1, y_2, \ldots, y_n]^{\mathrm{T}}$ are the outputs of slave system and $0 < \alpha_i < 1$, $i = 1, \ldots, n$ are the fractional derivatives orders. $D^{\alpha} y_i$ is the fractional derivative of y_i. The regular definitions for fractional derivatives are: Grünwald–Letnikov, Riemann–Liouville and Caputo definitions. For instance, the Caputo definition is given as:

$$D^{\alpha} y = \frac{1}{\Gamma(m-\alpha)} \int_0^t \frac{y^m(\tau)}{(t-\tau)^{\alpha-m+1}} \mathrm{d}\tau \tag{2}$$

where m is integer so that $m - 1 < \alpha < m$ and $\Gamma(\cdot)$ is Gamma function ($\Gamma(t) = \int_0^{\infty} x^{t-1} e^{-x} \mathrm{d}x$).

The master system is considered as follows:

$$\begin{aligned} D^{\beta_1} x_1 &= g_1(x_1, \ldots, x_n) \\ &\vdots \\ D^{\beta_n} x_n &= g_n(x_1, \ldots, x_n) \end{aligned} \tag{3}$$

where $g_i, i = 1, 2, \ldots, n$ are unknown but bounded functions, $\underline{x} = [x_1, x_2, \ldots, x_n]^{\mathrm{T}}$ are the outputs of master system, and $0 < \beta_i < 1$, $i = 1, \ldots, n$ are the fractional derivatives orders. The synchronization errors are defined as $e_i = y_i - x_i$, $i = 1, \ldots, n$. The control objective is to design controllers $u_i, i = 1, 2, \ldots, n$ such that $\|e_i\| \to 0 \; as \; t \to \infty$.

The proposed control block diagram for i-th subsystem is shown in Fig. 1. As shown in Fig. 1, the unknown function in the dynamics of the slave systems is estimated by the proposed self-evolving fuzzy system, and by using this fuzzy system, an error feedback controller is designed [see Eq. (6)]. Then, the synchronization problem [see Eq. (8)] is rewritten as a standard H_∞ problem [see Eqs. (22, 23)]. To show the robustness of the proposed control scheme and the stability analysis, a compensator is designed based on the H_∞ control technique [see u_{s_i} in Eq. (23)], by using the results of [14].

The i-th subsystem is considered as follows:

$$D^{\alpha_i} y_i = f_i(y_1, \ldots, y_n) + d_i(t) + u_i(t) \tag{4}$$

As shown in Fig. 1, the term $f_i(y_1, \ldots, y_n) + d_i(t)$ in (4) is estimated by SE-NT2FNN $\hat{f}_i$. The approximation error is defined as follows:

$$\varepsilon_i = f_i(y_1, \ldots, y_n) + d_i(t) - \hat{f}_i \tag{5}$$

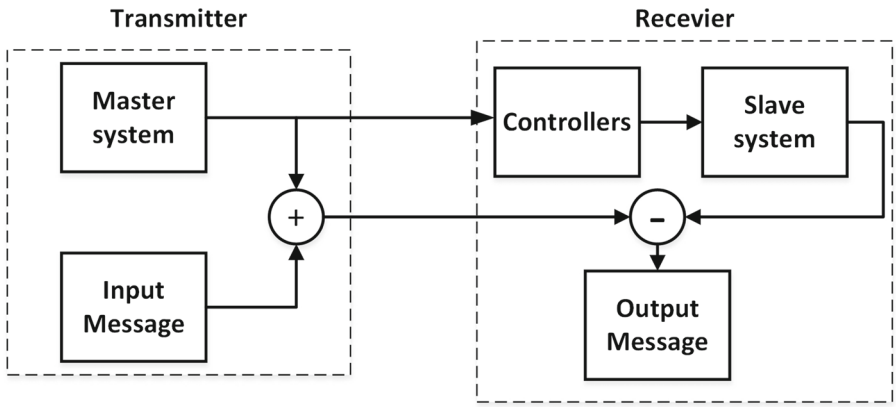

Fig. 2 The proposed secure communication scheme

We define u_i as $u_i = u_i^* + u_{s_i}$, in which u_i^* is designed as follows:

$$u_i^* = D^{\alpha_i} x_i - \lambda_i e_i - \hat{f}_i \tag{6}$$

where λ_i is chosen such that stability condition $|\arg(\lambda_i)| > \alpha_i \frac{\pi}{2}$ is satisfied. This stability condition is derived from the following theorem:

Theorem 1 ([35]) *The following linear autonomous system*

$$D^{\alpha} x = Ax \tag{7}$$

with $0 < \alpha \leq 1$, $x \in R^n$ *and* $A \in R^{n \times n}$ *is, is asymptotically stable if and only if all the eigenvalues of matrix A satisfy* $|\arg(eig\,(A))| > \alpha \frac{\pi}{2}$.

By substituting (6) into (4) we have:

$$D^{\alpha_i} e_i + \lambda_i e_i = \varepsilon_i + u_{s_i} \tag{8}$$

u_{s_i} is designed such that the H_∞ norm of closed-loop transfer function ($T_{e\varepsilon}$), from e_i to ε_i is minimized. The proposed synchronization method is used in a secure communication application. The proposed secure communication scheme is shown in Fig. 2. The input message is encrypted using signals of master hyperchaotic system and is sent to the receiver. In the receiver, after synchronization, the message signal hidden inside a hyperchaotic signal is recovered.

3 Proposed non-singleton type-2 fuzzy neural network

In this section, the structure of proposed SE-NT2FNN is introduced. As shown in Fig. 1, the unknown functions in the dynamics of the slave systems are estimated by the proposed SE-NT2FNN. The structure and the consequent parameters of SE-NT2FNN are online adjusted based on a proposed self-evolving algorithm and the gradient descent algorithm, respectively [see Sects. 4.1, 4.2]. As shown in Fig. 1, the training data are coming from the slave system at each sample time. The main merits of proposed SE-NT2FNN compared with other fuzzy neural networks are that the proposed fuzzy system has only one rule initially and new MFs and rules are added when necessary and also the unimportant rules are deleted based on a simple algorithm. Furthermore, the input uncertainties are handled by the proposed non-singleton fuzzification.

The proposed network structure has six layers as shown in Fig. 3.

Each rule has the following form:

$$Rule\ i: IF\ y_1\ is\ \tilde{A}_1^i\ And \cdots And\ y_n\ is\ \tilde{A}_n^i\ Then\ \hat{f} \in \left[w_l^i, w_r^i\right]\ \ i = 1, \ldots, M \tag{9}$$

where M is the number of rules, y_l, $l = 1, \ldots, n$ are inputs of SE-NT2FNN, n is the number of inputs of SE-NT2FNN, $\tilde{A}_j^i$ $j = 1, \ldots, n$ is the i-th interval type-2 membership function (MF) for the j-th input and $\left[w_l^i, w_r^i\right]$ are the consequent parameters. $\hat{f}$ is output of SE-NT2FNN. Each layer of SE-NT2FNN is explained as follows:

Input layer: The inputs of SE-NT2FNN are the outputs of slave system.

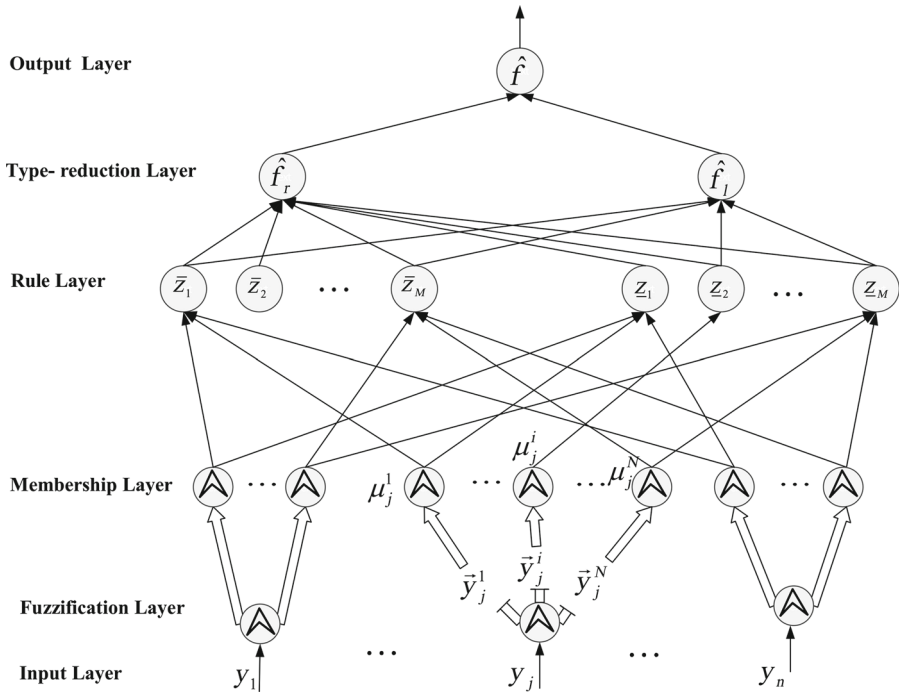

Fig. 3 Structure of SE-NT2FNN

Fuzzification layer: In this layer, the non-singleton fuzzification operation is performed. The uncertainties of inputs of SE-NT2FNN are modeled by type-2 MFs. The proposed type-2 MF for input y_j has three points, in which its first-point, center-point and end-point are located at $y_j-\Delta$, y_j and $y_j+\Delta$, respectively (as shown in Fig. 4). Δ is a designable parameter which is constant for all inputs. By this fuzzifier, crisp inputs are mapped into a type-2 MF. The non-singleton fuzzifier changes the membership values of MFs. Consider i-th MF for j-th input, the non-singleton fuzzifier transforms y_j to $\vec{y}_j^{\,i}$. By using minimum inference $\vec{y}_j^{\,i}$ is obtained as follows:

where y_j is j-th input, a_j^i, m_j^i and b_j^i are first-point, center-point and end-point of i-th MF for j-th input, respectively (Figs. 5, 6).

Membership layer: In this layer, the upper and lower memberships of MFs are computed. Consider i-th MF for j-th input y_j, the upper and lower memberships of $\vec{y}_j^{\,i}$ (transformed of y_j by non-singleton fuzzifier) are obtained as follows:

$$\vec{y}_j^{\,i}=\begin{cases} y_j \quad \text{if } \left(y_j+\Delta\right)<a_j^i \text{ or } \left(y_j-\Delta\right)>b_j^i \text{ or } y_j=m_j^i \\ \dfrac{\Delta\times a_j^i+\left|a_j^i-m_j^i\right|\times\left(y_j+\Delta\right)}{\Delta+\left|a_j^i-m_j^i\right|} \quad \text{else if } y_j<m_j^i \text{ see Fig. 5} \\ \dfrac{\Delta\times b_j^i+\left|b_j^i-m_j^i\right|\times\left(y_j-\Delta\right)}{\Delta+\left|b_j^i-m_j^i\right|} \quad \text{else if } y_j>m_j^i \text{ see Fig. 6} \end{cases} \tag{10}$$

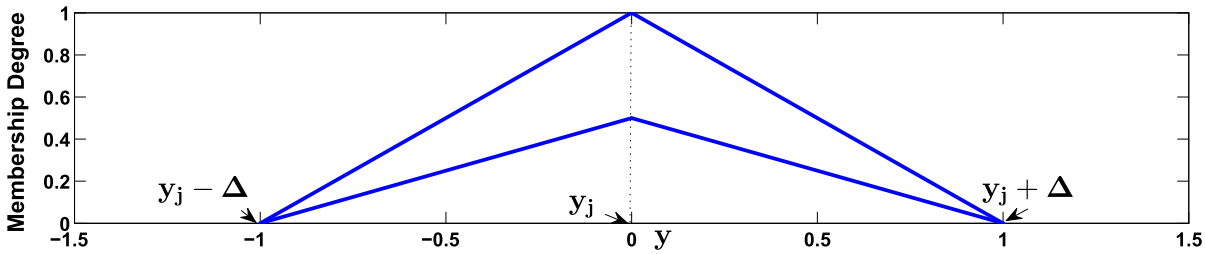

Fig. 4 Modeling of the uncertainty of inputs by proposed type-2 MF

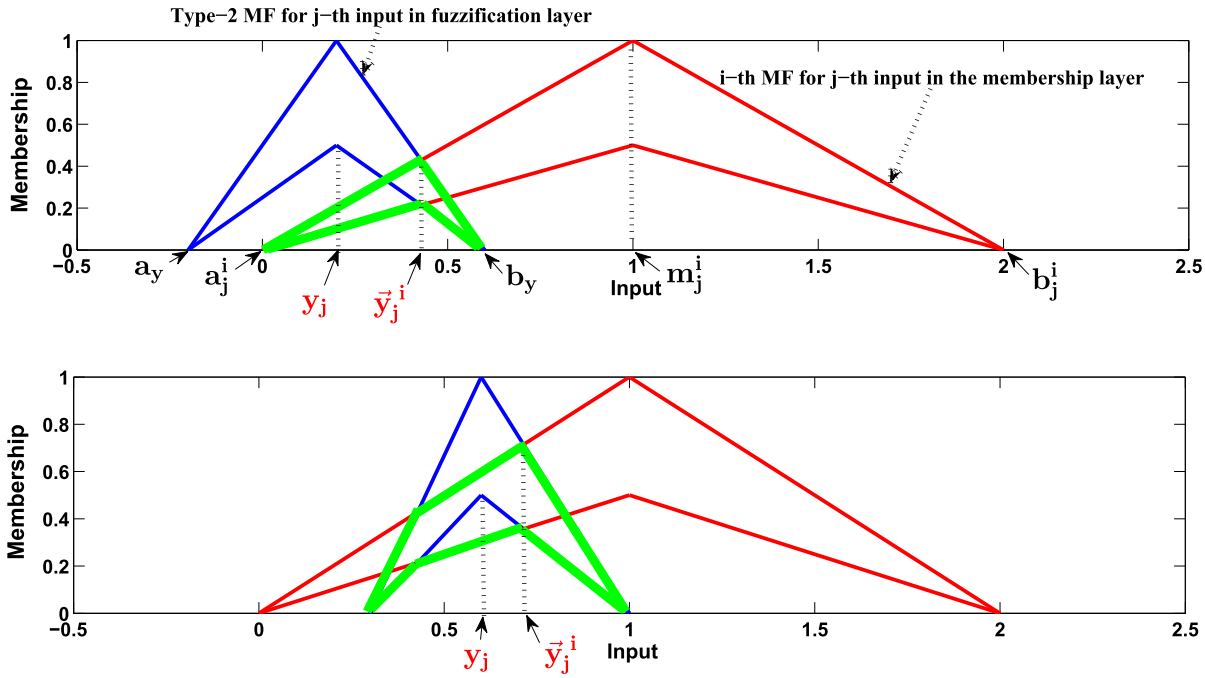

Fig. 5 Non-singleton fuzzifier by using minimum inference

$$\bar{\mu}^{i}_{\vec{y}^{i}_j} = \begin{cases} \dfrac{\vec{y}^{i}_j - a^{i}_j}{m^{i}_j - a^{i}_j} & \text{if} \quad a^{i}_j < \vec{y}^{i}_j \le m^{i}_j \\ \dfrac{\vec{y}^{i}_j - b^{i}_j}{m^{i}_j - b^{i}_j} & \text{if} \quad m^{i}_j < \vec{y}^{i}_j < b^{i}_j \\ 0 & \text{otherwise} \end{cases}$$

$$\underline{\mu}^{i}_{\vec{y}^{i}_j} = \begin{cases} 0.5\dfrac{\vec{y}^{i}_j - a^{i}_j}{m^{i}_j - a^{i}_j} & \text{if} \quad a^{i}_j < \vec{y}^{i}_j \le m^{i}_j \\ 0.5\dfrac{\vec{y}^{i}_j - b^{i}_j}{m^{i}_j - b^{i}_j} & \text{if} \quad m^{i}_j < \vec{y}^{i}_j < b^{i}_j \\ 0 & \text{otherwise} \end{cases} \tag{11}$$

Rule layer: Each node in this layer corresponds to a rule, which computes the upper and lower firing degrees. The upper and lower firing degrees of i-th rule are computed as follows:

$$\begin{aligned} \bar{z}_i &= \bar{\mu}^{p_1}_{\vec{y}_1^{p_1}} \times \bar{\mu}^{p_2}_{\vec{y}_2^{p_2}} \times \cdots \times \bar{\mu}^{p_j}_{\vec{y}_j^{p_j}} \times \cdots \times \bar{\mu}^{p_n}_{\vec{y}_n^{p_n}} \\ \underline{z}_i &= \underline{\mu}^{p_1}_{\vec{y}_1^{p_1}} \times \underline{\mu}^{p_2}_{\vec{y}_2^{p_2}} \times \cdots \times \underline{\mu}^{p_j}_{\vec{y}_j^{p_j}} \times \cdots \times \underline{\mu}^{p_n}_{\vec{y}_n^{p_n}} \end{aligned} \tag{12}$$

where $\bar{\mu}^{p_j}_{\vec{y}_j^{p_j}}$ and $\underline{\mu}^{p_j}_{\vec{y}_j^{p_j}}$ are the upper and lower memberships of p_j-th MF for j-th input, respectively.

Type-reduction layer: Based on the center of sets type reduction, $\hat{f}_r$ and $\hat{f}_l$ are as follows:

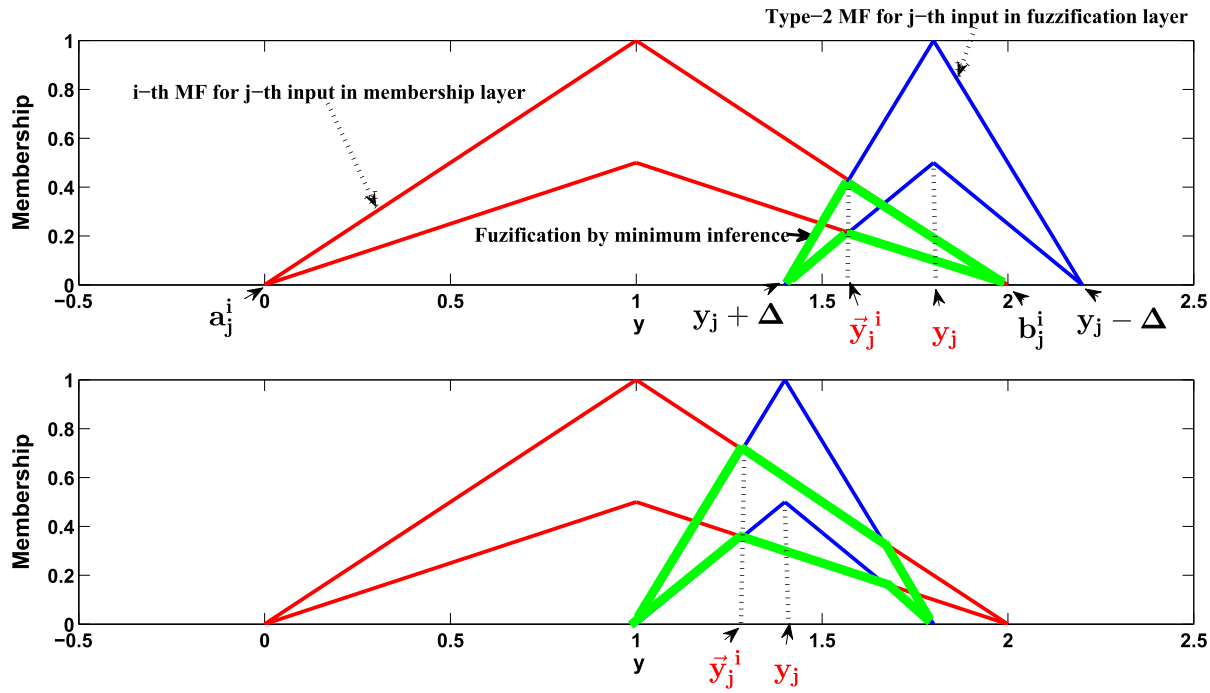

Fig. 6 Non-singleton fuzzifier by using minimum inference

$$\hat{f}_r = \frac{\sum_{j=1}^{R} \underline{z}_j w_r^j + \sum_{j=R+1}^{M} \bar{z}_j w_r^j}{\sum_{j=1}^{R} \underline{z}_j + \sum_{j=R+1}^{M} \bar{z}_j},$$
$$\hat{f}_l = \frac{\sum_{j=1}^{L} \bar{z}_j w_l^j + \sum_{j=L+1}^{M} \underline{z}_j w_l^j}{\sum_{j=1}^{L} \bar{z}_j + \sum_{j=L+1}^{M} \underline{z}_j} \tag{13}$$

in which R and L are obtained from KM iterative algorithm [36]. w_r^j and w_l^j are the consequent parameters. $\bar{z}_j$ and $\underline{z}_j$ are the upper and lower firing degrees of j-th rule, respectively, and M is the number of rules. To simplify Eq. (13), the following definitions are considered:

$$q_r \triangleq \left[\overbrace{1\ 1\cdots 1}^{R}\ \overbrace{0\ 0\cdots 0}^{M-R}\right]^{\mathrm{T}},$$
$$q_l \triangleq \left[\overbrace{1\ 1\cdots 1}^{L}\ \overbrace{0\ 0\cdots 0}^{M-L}\right]^{\mathrm{T}} \tag{14}$$

where $\overbrace{1\ 1\cdots 1}^{R}$ represent that the number of ones is R. According to (14), Eq. (13), can be rewritten as follows:

$$\hat{f}_r = \frac{\sum_{j=1}^{M} \left[q_r(j)\underline{z}_j + (1 - q_r(j))\,\bar{z}_j\right] \times w_r^j}{\sum_{j=1}^{M} \left[q_r(j)\underline{z}_j + (1 - q_r(j))\,\bar{z}_j\right]},$$
$$\hat{f}_l = \frac{\sum_{j=1}^{M} \left[q_l(j)\bar{z}_j + (1 - q_l(j))\,\underline{z}_j\right] w_l^j}{\sum_{j=1}^{M} \left[q_l(j)\bar{z}_j + (1 - q_l(j))\,\underline{z}_j\right]} \tag{15}$$

where $q_r(j)$ and $q_l(j)$ represent the j-th element of vector q_r and q_l, respectively. *Output layer*: The defuzzified crisp output $\hat{f}$ is the average of $\hat{f}_r$ and $\hat{f}_l$:

$$\hat{f} = \frac{\hat{f}_r + \hat{f}_l}{2} \tag{16}$$

4 Self-evolving algorithm

In this section, consequent parameters [see Eq. (13)] and the structure of type-2 fuzzy neural network are tuned.

4.1 Parameter learning

The consequent parameters w_r^j, w_l^j, $j = 1, \ldots, M$ are tuned based on gradient descent algorithm. As shown in Fig. 1, the parameters w_r^j, w_l^j, $j = 1, \ldots, M$ are tuned such that the following cost function is minimized:

$$E = \frac{1}{2}\left[y_i - D^{-\alpha_i}\left(\hat{f}_i + u_i\right)\right]^2 \tag{17}$$

where y_i is the output of i-th subsystem, $D^{-\alpha_i}$ is fractional integrator, $\hat{f}_i$ is the output of i-th SE-NT2FNN and u_i is i-th control signal in i-th subsystem. Based on gradient descent algorithm, we have:

$$\begin{aligned} w_r^j(t+1) &= w_r^j(t) - \eta \frac{\partial E}{\partial w_r^j} \\ &= w_r^j(t) - \eta \frac{\partial E}{\partial \hat{f}_i} \frac{\partial \hat{f}}{\partial w_r^j} \\ &= w_r^j(t) \\ &\quad + \eta \left[y_i - D^{-\alpha_i} \left(\hat{f}_i + u_i \right) \right] D^{-\alpha_i} \\ &\quad \times \left(\frac{q_r(j) \underline{z}_j + (1 - q_r(j)) \bar{z}_j}{\sum_{j=1}^{M} \left[q_r(j) \underline{z}_j + (1 - q_r(j)) \bar{z}_j \right]} \right) \end{aligned} \tag{18}$$

Similar to (18), for training of w_l^j we have:

$$\begin{aligned} & w_l^j(t+1) \\ &= w_l^j(t) + \eta \left[y_i - D^{-\alpha_i} \left(\hat{f}_i + u_i \right) \right] D^{-\alpha_i} \\ &\quad \times \left(\frac{q_l(j) \bar{z}_j + (1 - q_l(j)) \underline{z}_j}{\sum_{j=1}^{M} \left[q_l(j) \bar{z}_j + (1 - q_l(j)) \underline{z}_j \right]} \right) \end{aligned} \tag{19}$$

4.2 Structure learning

In this section, a new structure learning algorithm is presented. Our proposed SE-NT2FNN has only one rule initially. New rules and new MFs are added, and unnecessary rules and MFs are deleted, when necessary. And the proposed algorithm limits the number of rules from indefinitely growing. The flowchart of proposed algorithm is shown in Fig. 7. When tracking error is greater than a predefined threshold, the structure is changed. Detailed explanation is given in the following.

4.2.1 Adding new MF

Consider input y_j, at time t, if the maximum of upper memberships of all MFs to input y_j is less than 0.5, a new MF is added for input y_j as shown in Fig. 8. The center-point of new MF m_j^{new} is located at y_j, its first-point a_j^{new} is chosen as center-point of neighboring MF and its end-point b_j^{new} is chosen as $b_j^{\text{new}} = 2 \times m_j^{\text{new}} - a_j^{\text{new}}$. It must be noted that each input has only one type-2 MF initially.

4.2.2 Replacing new MF

Consider input y_j, if the number of MFs for input y_j is greater than a predefined threshold, after adding new MF, the furthest MF from newly added MF is deleted.

4.2.3 Generate new rules

After adding or replacing new MFs, all new rules, the firing degrees of which are greater than 0.5 are generated. Let the current SE-NT2FNN output value be w, the consequent parameters of new rules w_r^{new}, w_l^{new} are initialized, as follows:

$$\begin{cases} w_r^{\text{new}} = w \ , \ w_l^{\text{new}} = 0 & w >= 0 \\ w_r^{\text{new}} = 0 \ , \ w_l^{\text{new}} = w & w < 0 \end{cases} \tag{20}$$

If by adding or replacing new MFs, there is no a new rule the firing degree of which is greater than 0.5, or there is not any rule in the rule database, the firing degree of which is greater than 0.5 , then a new rule is generated as follows:

For each input, one MF is found which its upper membership is maximum. The center of this MF is changed to the current input value. Also the end-point of left neighboring MF and the first-point of right neighboring MF are modified to the current input value [see Fig. 9].

For example, assume y_1, y_2 and y_3 are the inputs of SE-NT2FNN, $\tilde{A}_{y_1}^1$, $\tilde{A}_{y_1}^2$, $\tilde{A}_{y_1}^3$ are the type-2 MFs for input y_1, $\tilde{B}_{y_2}^1$, $\tilde{B}_{y_2}^2$, $\tilde{B}_{y_2}^3$ are the type-2 MFs for input y_2 and $\tilde{C}_{y_3}^1$, $\tilde{C}_{y_3}^2$, $\tilde{C}_{y_3}^3$ are the type-2 MFs for input y_3 . And assume the output of SE-NT2FNN at time t is w. If the center of MFs $\tilde{A}_{y_1}^1$, $\tilde{B}_{y_2}^3$ and $\tilde{C}_{y_3}^2$ are changed [see Fig. 9], the new rule is generated as follows:

If y_1 is $\tilde{A}_{y_1}^1$, and y_2 is $\tilde{B}_{y_2}^3$, and y_3 $\tilde{C}_{y_3}^2$, Then $\hat{f}$ is $\tilde{G}$ Centroid of $\tilde{G}$ is $[w_l, w_r]$ where

$$\begin{cases} w_r = w, & w_l = 0 \quad \text{if} \quad w \geq 0 \\ w_r = 0, & w_l = w \quad \text{if} \quad w < 0 \end{cases} \tag{21}$$

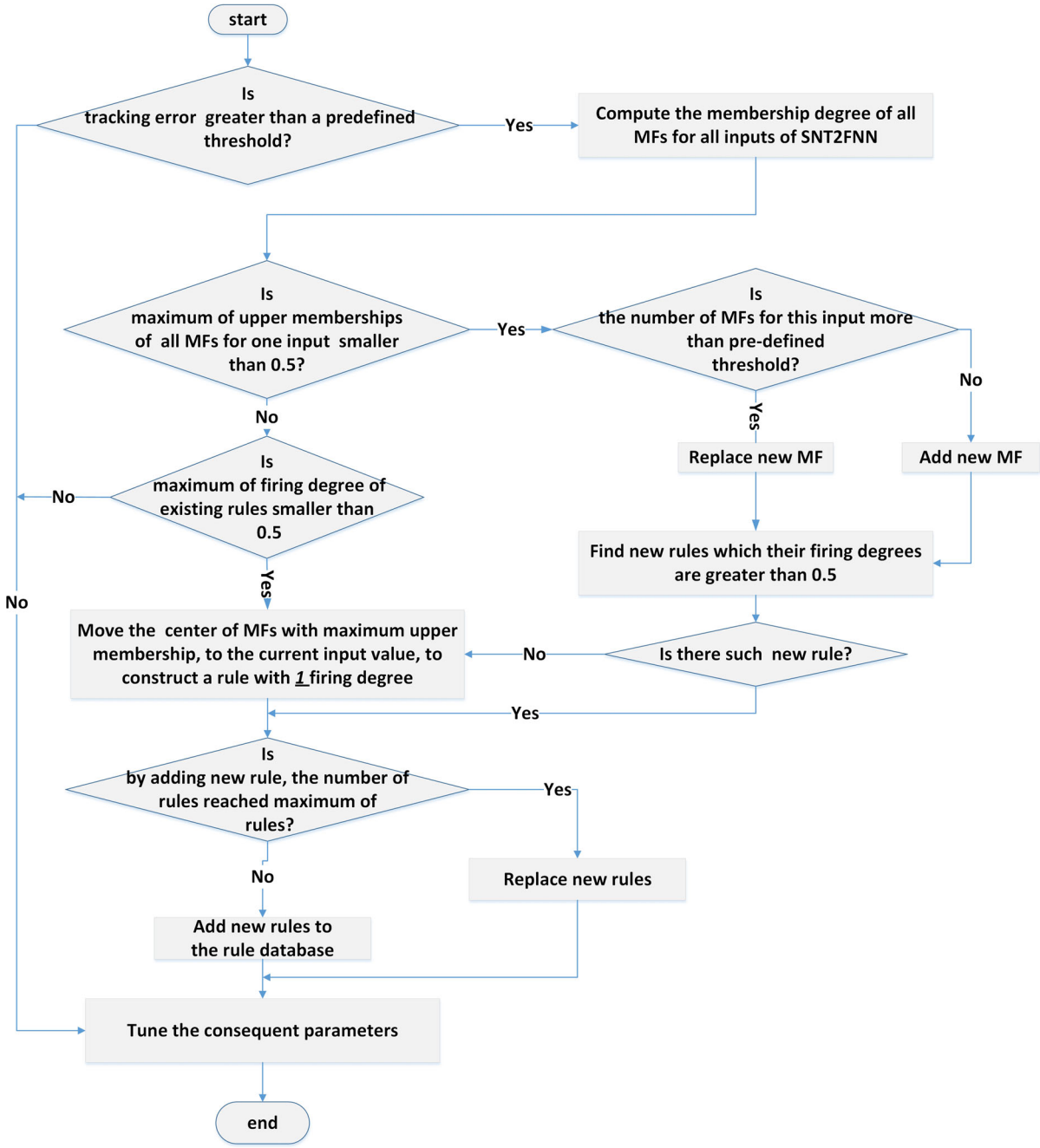

Fig. 7 Proposed structure learning algorithm

4.2.4 Add new rules to the rule database

If by adding new rules to the rule database, the number of rules is greater than a predefined threshold (maximum number of rules), the new generated rules are replaced with the rules which have the smallest firing degrees. Otherwise, new rules are added to rule database. It must be noted that since the consequent parameters of new rules are initialized to SE-NT2FNN current output value, the control signal remains continues,

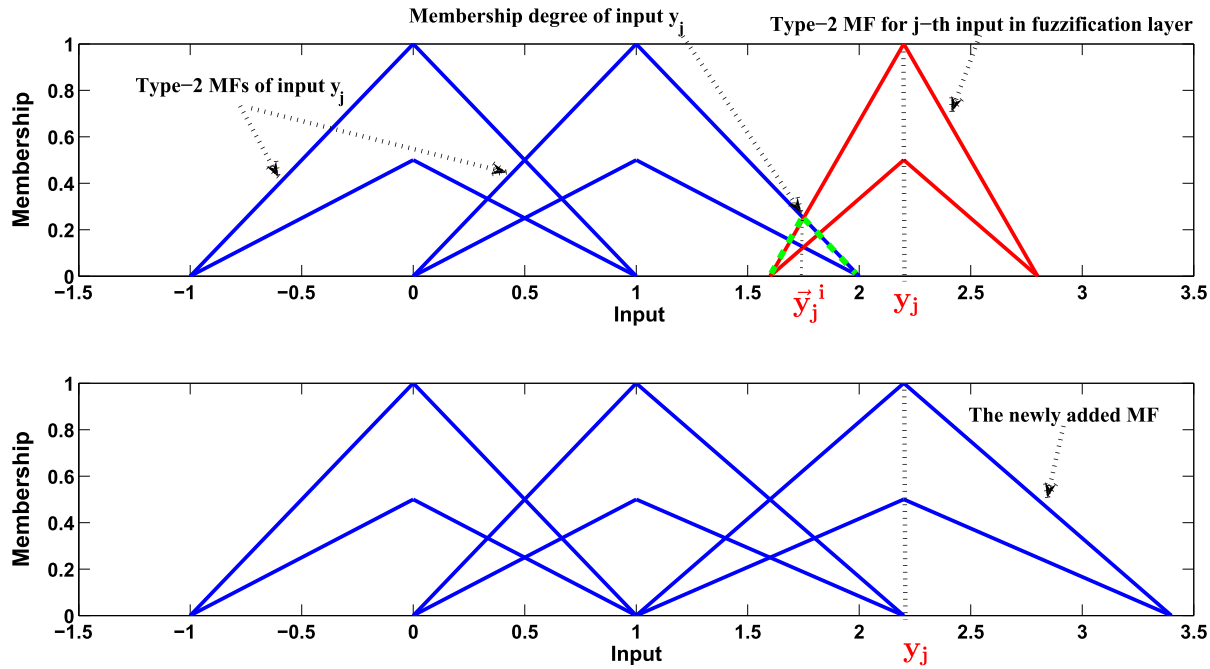

Fig. 8 Adding new MF for input y_j

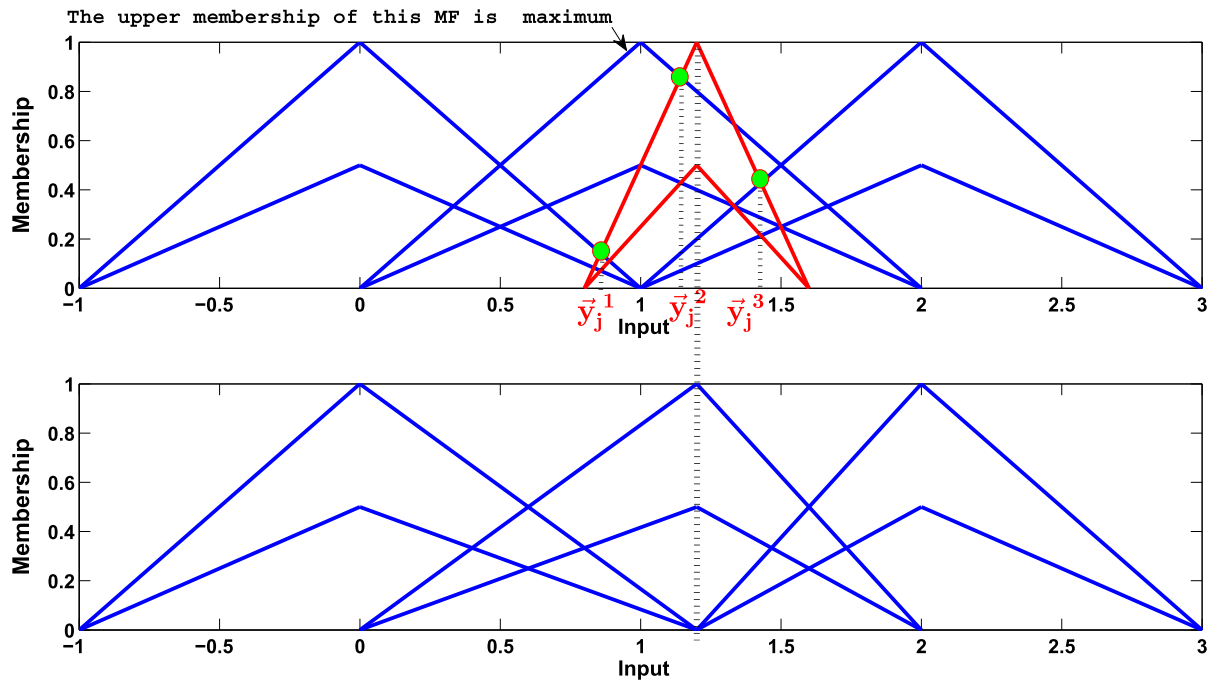

Fig. 9 Change the center of one MF which its upper membership is maximum

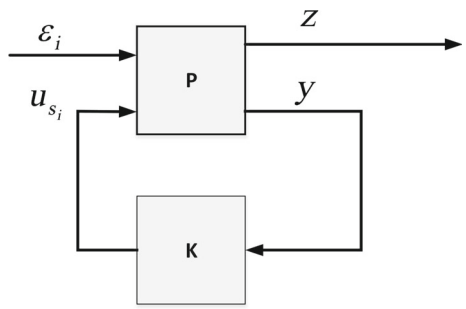

Fig. 10 Configuration of standard H_∞ problem

and then, our assumption about bounded approximation error remains valid. So the stability analysis are valid when the structure changes.

5 Stability analysis

In this section, a compensator is designed such that H_∞ norm of transfer function $T_{e\varepsilon}$ is minimized. We represent the Eq. (8) as a standard H_∞ problem as shown in Fig. 10.

where,

$$P\begin{cases} D^{\alpha_i} e_i = Ae_i + Bu_{s_i} + B_\varepsilon \varepsilon_i \\ y = Ce_i + Du_{s_i} + D_\varepsilon \varepsilon_i \\ z = C_z e_i + D_z u_{s_i} + D_{z\varepsilon}\varepsilon_i \end{cases} \tag{22}$$

$$K\begin{cases} D^{\alpha_i} x_k = A_k x_k + B_k y \\ u_{s_i} = C_k x_k + D_k y \end{cases} \tag{23}$$

in which, $A = -\lambda_i$, $B = 1$, $B_\varepsilon = 1$, $C = 1$, $D = 0$, $D_\varepsilon = 0$, $C_z = 1$, $D_z = 0$, $D_{z\varepsilon} = 0$, $e_i \in R^n$ is the state of subsystem (8), $u_i \in R^{n_u}$ is control signal, $y \in R^{n_y}$ and $z \in R^{n_z}$ are outputs and $x_k \in R^n$ is the state of controller.

With definition $\tilde{x}(t) = \left[e_i \; x_k\right]^{\mathrm{T}}$, the state-space representation of the closed-loop $T^{cl}_{z\varepsilon_i}$ can be written as follows:

$$T^{cl}_{z\varepsilon_i} = \begin{cases} D^{\alpha_i}\tilde{x} = A_{cl}\tilde{x} + B_{cl}\varepsilon_i \\ z = C_{cl}\tilde{x} + D_{cl}\varepsilon_i \end{cases} \tag{24}$$

where

$$A_{cl} = \begin{bmatrix} A + BD_kC & BC_k \\ B_kC & A_k \end{bmatrix},\; B_{cl} = \begin{bmatrix} B_\varepsilon + BD_kD_\varepsilon \\ B_kD_\varepsilon \end{bmatrix}$$
$$C_{cl} = \begin{bmatrix} C_z + D_zD_kC & D_zC_k \end{bmatrix},\; D_{cl} = D_{z\varepsilon} + D_zD_kD_\varepsilon \tag{25}$$

Various methods have been presented for computation of the upper bound of H_∞-norm.

Lemma 1 ([37,38]): *The H_∞-norm of system (24), is bounded by γ, if and only if there exists symmetric positive definite $X = X^* \in R^{2n\times 2n}$ such that:*

$$\begin{bmatrix} \bar{r}A_{cl}^T X + Xr A_{cl} & XB_{cl} & \bar{r}C_{cl}^T \\ B_{cl}^T X & -\gamma^2 I & D_{cl}^T \\ rC_{cl} & D_{cl} & -\gamma I \end{bmatrix} < 0 \tag{26}$$
$$with \;\; r = e^{(1-\alpha_i)j\pi/2}$$

Partition the solution of (26) as follows:

$$X = \begin{bmatrix} Y & N \\ N^T & * \end{bmatrix},\; X^{-1} = \begin{bmatrix} Z & M \\ M^T & * \end{bmatrix} \tag{27}$$

in which, Z and Y are symmetric and $n \times n$. By using (26) and linearizing change of variables, Theorem 2, [14] has been derived:

Theorem 2 ([14]): *The fractional-order system (22) with $1 < \alpha_i < 2$, by output feedback control (23), is Bounded-Input Bounded-Output (BIBO) stabilizable and $\left\|T^{cl}_{zw}\right\| < \gamma$, if there exist $Z = Z^T \in R^{n\times n}$, $Y = Y^T \in R^{n\times n}$, $\hat{A} \in R^{n\times n}$, $\hat{B} \in R^{n\times n_y}$, $\hat{C} \in R^{n_u\times n}$ and $\hat{D} \in R^{n_u\times n_y}$ such that LMI (29) is feasible with*

$$\begin{bmatrix} Z & I \\ I & Y \end{bmatrix} \succ 0 \tag{28}$$

$$\begin{bmatrix} \bar{r}\left(AZ+B\hat{C}\right)+r\left(ZA^T+\hat{C}^TB^T\right) & \bar{r}\left(YA+\hat{B}C\right)+r\left(A^TY+C^T\hat{B}^T\right) & B_w+B\hat{D}D_w & \bar{r}\left(C_zZ+D_z\hat{C}\right)^T \\ r\left(A+B\hat{D}C\right)^T+\bar{r}\hat{A} & \left(YB_w+\hat{B}D_w\right)^T & YB_w+\hat{B}D_w & \bar{r}\left(C_z+D_z\hat{D}C\right)^T \\ \left(B_w+B\hat{D}D_w\right)^T & r\left(C_z+D_z\hat{D}C\right) & -\gamma^2 I & \left(D_{zw}+D_z\hat{D}D_w\right)^T \\ r\left(C_zZ+D_z\hat{C}\right) & \bar{r}\left(YA+\hat{B}C\right)+r\left(A^TY+C^T\hat{B}^T\right) & D_{zw}+D_z\hat{D}D_w & -I \end{bmatrix} < 0 \tag{29}$$

where

$$\begin{aligned} \hat{A} &\triangleq NA_kM^T+NB_kCZ+YBC_kM^T+Y(A+BD_kC)Z \\ \hat{B} &\triangleq NB_k+YBD_k \\ \hat{C} &\triangleq C_kM^T+D_kCZ \\ \hat{D} &\triangleq D_k \end{aligned} \tag{30}$$

The results of Theorem 2 is derived from [38] and can be easily extended to case of fractional-order system (22) with $0 < \alpha_i < 1$.

After solving (29), matrices M and N must be find such that:

$$MN^T = I - ZY \tag{31}$$

By using (31) and (30), the controller matrices A_k, B_k, C_k, D_k can be derived as follows:

$$\begin{aligned} D_k &\triangleq \hat{D} \\ C_k &\triangleq \left(\hat{C}-D_kCX\right)M^{-T} \\ B_k &\triangleq N^{-1}\left(\hat{B}-YBD_k\right) \\ A_k &\triangleq N^{-1}(\hat{A}-NB_kCX-YBC_kM^T-Y(A+BD_kC)X)M^{-T} \end{aligned} \tag{32}$$

6 Simulations

In this section, two examples are presented to evaluate the performance of proposed controller for the synchronization of uncertain fractional hyperchaotic systems and its application to secure communication.

Many numerical methods, based on the approximation of fractional derivative (integral) operators, have been presented for solving the fractional differential Eqs. [39–42]. In this paper, for simulation the Caputo derivative of fractional-order, we use Simulink block *nid*, which has been created by Duarter Valerio [43]. The use of Caputo derivative is more popular in real applications.

Example 1 In this example, the proposed controller is applied to synchronize the fractional-order hyperchaotic Novel system and fractional-order hyperchaotic Chen system [44]. The master and slave systems dynamics are given as follows:

$$\text{Master system:} \begin{cases} D^{\beta_1}x_1 = 35(x_2-x_1)+35x_2x_1 \\ D^{\beta_2}x_2 = 25x_1-5x_1x_3+x_2+x_4 \\ D^{\beta_3}x_3 = x_1x_2-4x_3 \\ D^{\beta_4}x_4 = -100x_2 \end{cases} \tag{33}$$

and

$$\text{Slave system:} \begin{cases} D^{\alpha_1}y_1 = 35(y_2-y_1)+y_4+d_1+u_1 \\ D^{\alpha_2}y_2 = 7y_1-y_1y_3+12y_2+d_2+u_2 \\ D^{\alpha_3}y_3 = y_1y_2-3y_3+d_3+u_3 \\ D^{\alpha_4}y_4 = y_2y_3+0.3y_4+d_4+u_4 \end{cases} \tag{34}$$

where $u_i, i = 1,2,3,4$ are controllers, $d_i, i = 1,2,3,4$ are external disturbance which are considered to be white noise with zero mean and variance 0.1. The fractional derivative orders are $\alpha_i = \beta_i = 0.97, i = 1,\ldots,4$. Initial conditions are chosen as $x_1(0) = 1$, $x_2(0) = 1$, $x_3(0) = 1$, $x_4(0) = 1$, $y_1(0) = 0.61$, $y_2(0) = 0.21$, $y_3(0) = 0.61$ and $y_4(0) = 0.21$. The parameters of self-evolving algorithm are given in Table 1. The input message is considered as $\sin(t)$.

To design the controller, we rewrite slave system (34) as follows:

Table 1 Parameters of self-evolving algorithm

Maximum number of rules	Maximum number of MFs for each input	The structure is changed when the tracking error greater than:	Δ see Fig. 4	Initial type-2 MF for each input: first-point, center-point, end-point
20	5	0.5	0.1	−10,0,10

$$\begin{aligned} D^{\alpha_1} y_1 &= f_1\left(\underline{y}\right) + u_1 \\ D^{\alpha_2} y_2 &= f_2\left(\underline{y}\right) + u_2 \\ D^{\alpha_3} y_3 &= f_3\left(\underline{y}\right) + u_3 \\ D^{\alpha_4} y_4 &= f_4\left(\underline{y}\right) + u_4 \end{aligned} \tag{35}$$

in which $\underline{y} = [y_1, y_2, y_3, y_4]$ and f_1, f_2, f_3, f_4 are nonlinear and unknown but bounded functions. The controllers u_1, u_2, u_3, u_4 are designed as follows:

$$\begin{aligned} u_1 &= D^{\alpha_1} x_1 - \lambda_1 e_1 - \hat{f}_1 + u_{s_1} \\ u_2 &= D^{\alpha_2} x_2 - \lambda_2 e_2 - \hat{f}_2 + u_{s_2} \\ u_3 &= D^{\alpha_3} x_3 - \lambda_3 e_3 - \hat{f}_3 + u_{s_3} \\ u_4 &= D^{\alpha_4} x_4 - \lambda_4 e_4 - \hat{f}_4 + u_{s_4} \end{aligned} \tag{36}$$

where $\hat{f}_i$, $i = 1, 2, 3, 4$ are SE-NT2FNNs which estimate $f_i(\underline{y}) + d_i(t)$, $i = 1, 2, 3, 4$ [see Fig. 1]. By substituting (36) into (34), we have:

$$\begin{aligned} D^{\alpha_1} e_1 &= -\lambda_1 e_1 + \varepsilon_1 + u_{s_1} \\ D^{\alpha_2} e_2 &= -\lambda_2 e_2 + \varepsilon_2 + u_{s_2} \\ D^{\alpha_3} e_3 &= -\lambda_3 e_3 + \varepsilon_3 + u_{s_3} \\ D^{\alpha_4} e_4 &= -\lambda_4 e_4 + \varepsilon_4 + u_{s_4} \end{aligned} \tag{37}$$

where ε_i , $i = 1, 2, 3, 4$ are approximation errors [see Eq. (5)], by considering $\lambda_i = 100$, $i = 1, 2, 3, 4$, after solving LMI (29), the matrices of controllers u_{s_i}, $i = 1, 2, 3, 4$ [see Fig. 10 and Eq. (23)] are obtained as follows:

$$\begin{cases} A_{k_i} = -18.4916, \ B_{k_i} = -1.3122 \\ C_{k_i} = 8.4653, \ D_{k_i} = 99.2928 \\ \gamma^2 = 0.7602 \end{cases} \tag{38}$$

Output trajectory of x_i and $y_i, i = 1, 2, 3, 4$ is shown in Fig. 11. The results of the encryption and decryption are shown in Fig. 12. It can be seen that the synchronization performance is desired, and the input message is recovered with a good accuracy. The fractional-order hyperchaotic systems of this example have been synchronized in [44], by a new nonlinear technique. The comparison values of root-mean-square error (RMSE) are given in Table 2. It can be seen that RMSE values for the synchronization error of our method are significantly less than [44]. It must be noted that dynamic of slave and master systems is assumed to be unknown in our method, and furthermore, external disturbance has been considered. But in [44], dynamic of slave and master system assumed to be known, and there is no external disturbance.

Example 2 In this example, the proposed controller is applied to synchronize the uncertain fractional-order hyperchaotic Lorenz system as the slave system, and fractional-order hyperchaotic Chen system as the master system. The hyperchaotic Lorenz system is as follows:

$$\begin{aligned} D^{\alpha} y_1 &= 10\,(y_2 - y_1) + y_4 + d_1^s + u_1 \\ D^{\alpha} y_2 &= 28 y_1 - y_2 - y_1 y_3 + d_2^s + u_2 \\ D^{\alpha} y_3 &= y_1 y_2 - 8/3 y_3 + d_3^s + u_3 \\ D^{\alpha} y_4 &= -y_2 y_3 - y_4 + d_4^s + u_4 \end{aligned} \tag{39}$$

Hyperchaotic chen system is:

$$\begin{aligned} D^{\beta} x_1 &= 35\,(x_2 - x_1) + x_4 + d_1^m \\ D^{\beta} x_2 &= 7x_1 + 12x_2 - x_1 x_3 + d_2^m \\ D^{\beta} x_3 &= x_1 x_2 - 8x_3 + d_3^m \\ D^{\beta} x_4 &= x_2 x_3 + 0.3x_4 + d_4^m \end{aligned} \tag{40}$$

where [45]

$$\begin{aligned} d_1^s &= 0.25\cos(6t) y_1 - 0.15\sin(t), \\ d_1^m &= -0.25\sin(4t) x_1 + 0.1\sin(7t) \\ d_2^s &= -0.2\cos(2t) y_2 + 0.1\sin(3t), \\ d_2^m &= 0.1\cos(t) x_2 + 0.15\cos(3t) \\ d_3^s &= 0.15\sin(3t) y_3 + 0.2\cos(5t), \end{aligned} \tag{41}$$

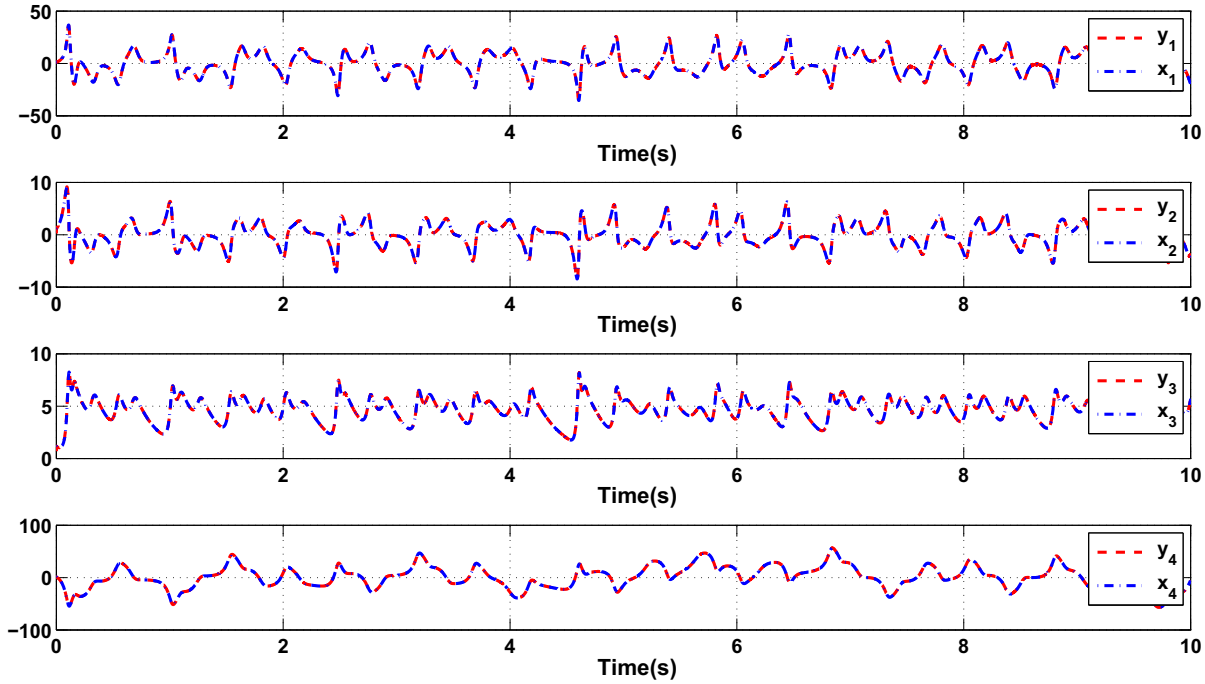

Fig. 11 Output trajectory of master and slave systems, Example 1

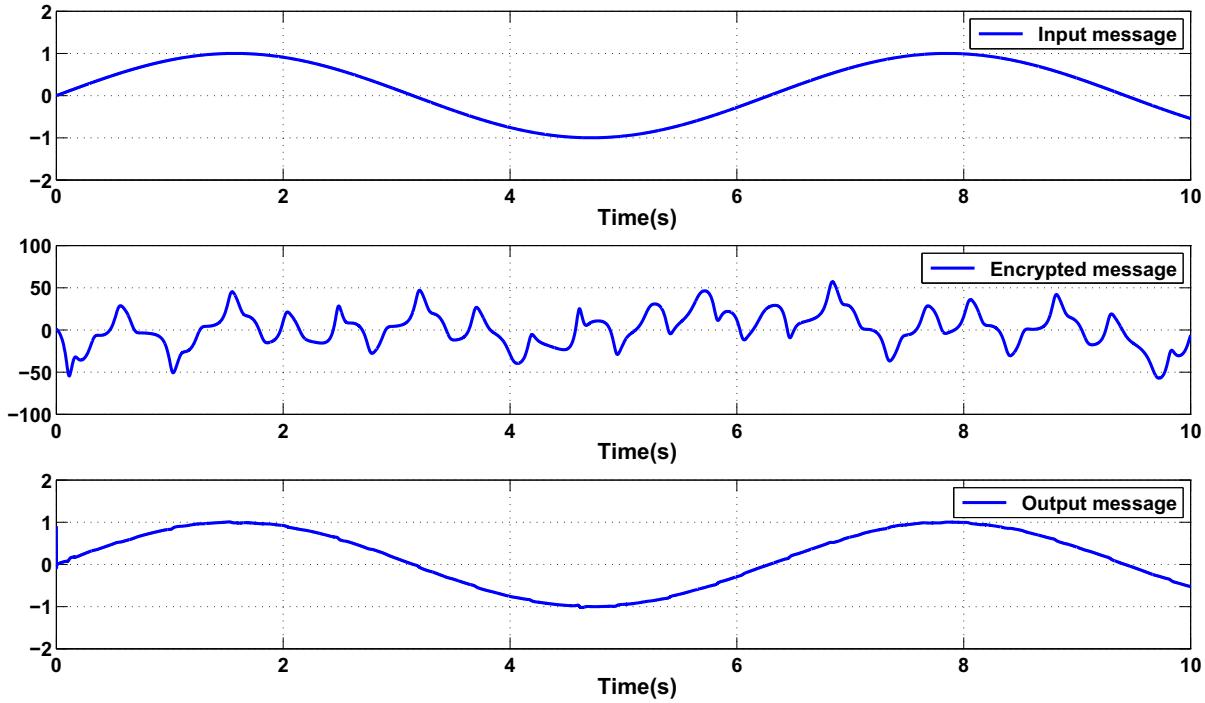

Fig. 12 Results for the encryption and decryption, Example 1

Table 2 Comparison results of proposed method in this paper and the proposed nonlinear technique in [44], Example 1

	RMSE			
	e_1	e_2	e_3	e_4
Proposed method	0.1599	0.0229	0.0145	0.0064
The method of [44]	1.5884	3.9767	2.5956	13.3590

$$d_3^m = 0.25\sin(4t)x_3 - 0.15\sin(5t)$$
$$d_4^s = -0.2\cos(2t)y_4 - 0.15\cos(t),$$
$$d_4^m = -0.15\sin(t)x_4 + 0.2\cos(2t)$$

Initial conditions of master and slave systems are as $y_1(0) = 1$, $y_2(0) = 2$, $y_3(0) = 3$, $y_4(0) = 4$, $x_1(0) = 3, x_2(0) = 1, x_3(0) = 4$ and $x_4(0) = -1$. The fractional derivative orders are $\alpha_i = \beta_i = 0.98\,, i = 1, \ldots, 4$. Other controller parameters are the same as the Example 1. The synchronization performance is shown in Fig. 13. The results of the encryption and decryption are shown in Fig. 14. The comparison results of proposed method and fractional non-singular terminal sliding mode technique [45] are given Table 3. It can be seen that the proposed controller shows better performance.

Example 3 In this example, the proposed controller is applied for synchronization of two uncertain fractional-order Liu systems with different initial conditions. The obtained results are compared with the results of [46]. In [46], the synchronization of two fractional-order Liu systems has been used in a secure communication scheme. The Liu system is as follows:

$$\begin{aligned} D^\alpha y_1 &= 10\,(y_2 - y_1) \\ D^\alpha y_2 &= 40y_1 - y_1 y_3 \\ D^\alpha y_3 &= -4y_1^2 - 2.5y_3 \end{aligned} \tag{42}$$

where $\alpha = 0.9$, the initial conditions of master and slave systems are $y_1(0), y_2(0), y_3(0) = (2, 1, 3)$ and $y_1(0), y_2(0), y_3(0) = (15, 6.5, 7)$ [46]. The input mes-

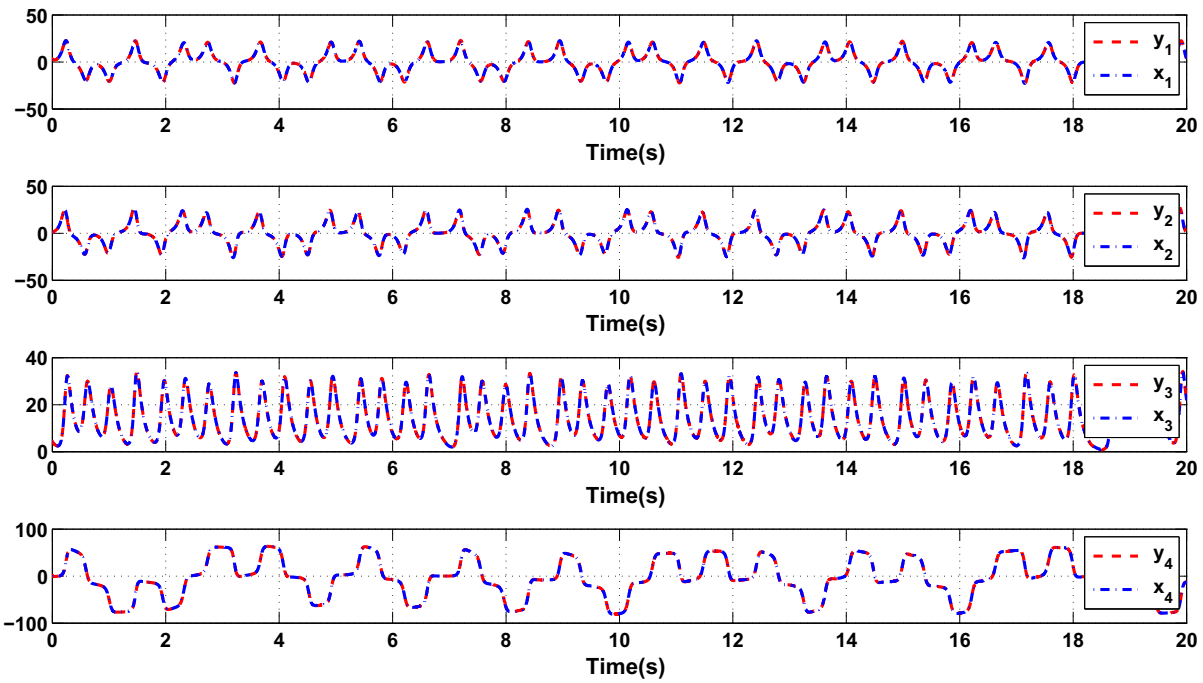

Fig. 13 Output trajectory of master and slave systems, Example 2

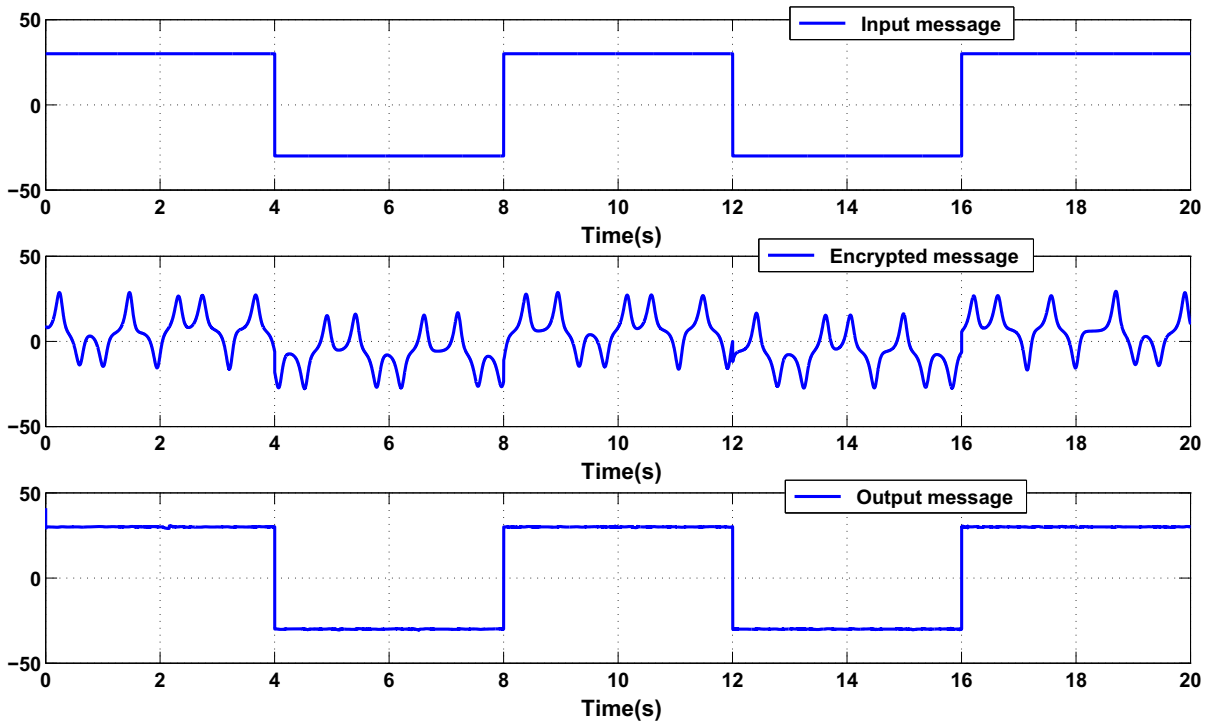

Fig. 14 Results for the encryption and decryption, Example 2

Table 3 Comparison results of proposed method in this paper and fractional non-singular terminal sliding mode technique [45], Example 2

	RMSE			
	e_1	e_2	e_3	e_4
Proposed method	0.0291	0.0680	0.1533	0.2707
The results of [44]	0.3342	0.2104	0.1972	1.7383

sage is considered as $sin(t)$. Other controller parameters are the same as the Example 1. The synchronization performance is shown in Fig. 15. The results of the encryption and decryption are shown in Fig. 16. The comparison results of proposed method and the method of [46] are given in Table 4. As the same as the previous examples, this example also shows that the proposed controller shows better performance. It must be noted that the image encryption based on the fractional-order chaotic systems has been studied in many papers. For instance in [47,48] the image encryption scheme are proposed based on a fractional-order chaotic logistic systems.

7 Conclusion

A new robust control strategy is proposed in this paper for synchronization of fractional-order hyperchaotic systems. Furthermore, a new self-evolving nonsingleton type-2 fuzzy neural network (SE-NT2FNN) presented, in which the structure of fuzzy neural network is not fixed and is modified when necessary and the proposed SE-NT2FNN has ability to identify dynamic of hyperchaotic systems. The effect of approximation error and external disturbance can be eliminated by H_∞ LMI-based control approach. It is shown that the closed-loop system is stable. The pro-

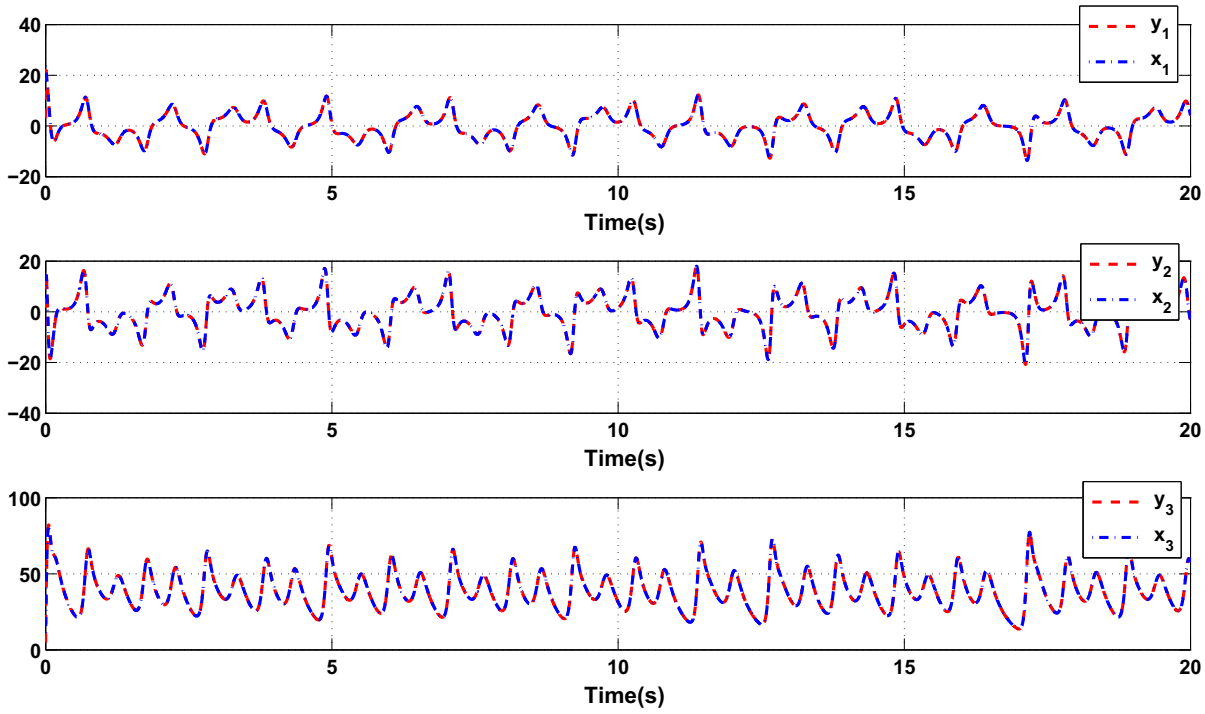

Fig. 15 Output trajectory of master and slave systems, Example 3

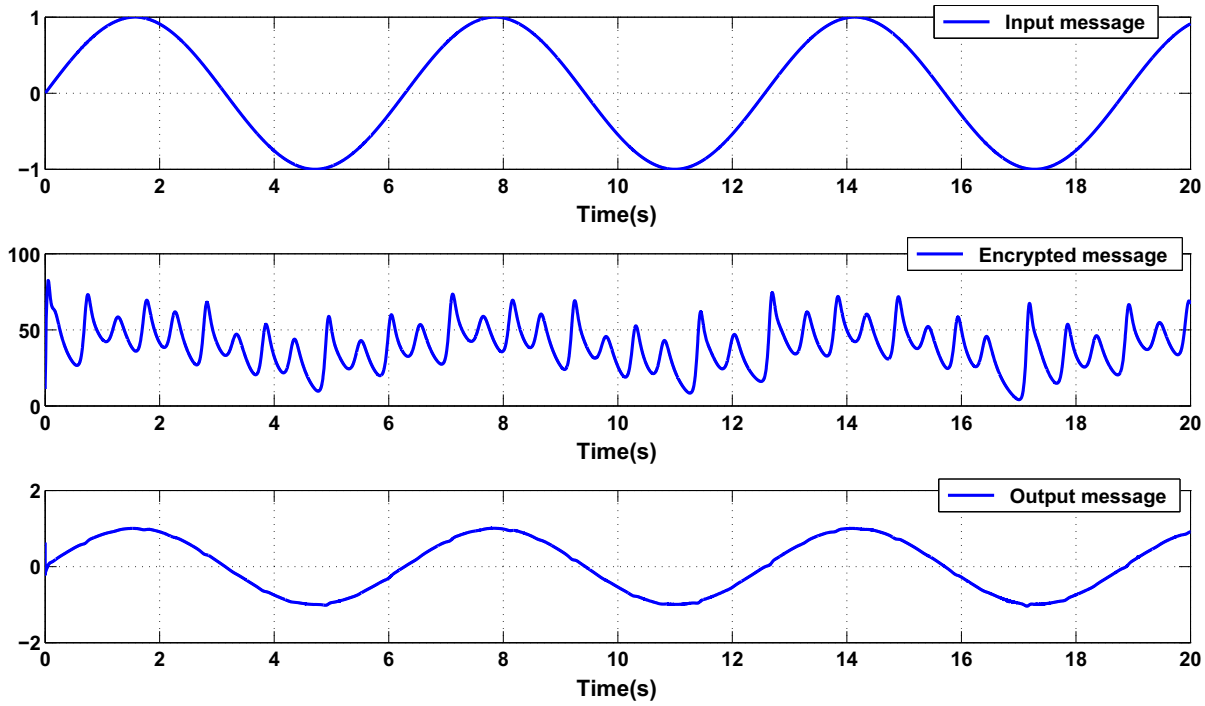

Fig. 16 Results for the encryption and decryption, Example 3

Table 4 Comparison of our results and the results of [46], Example 3

	RMSE		
	e_1	e_2	e_3
Proposed method	0.1754	0.0845	0.1187
The method of [46]	3.3043	1.1299	1.1347

posed method is successfully applied to synchronize two identical and nonidentical fractional-order hyperchaotic systems. The simulation results verified that proposed controller shows good performance in the presence of unknown functions and external disturbances. Also the results for the encryption and decryption of the input message in the secure communication system, confirmed the effectiveness of the proposed synchronization scheme. As we know, in all of works in the field of synchronization of the fractional-order chaotic systems and also in this paper, the value of the fractional-order is assumed to be known. In the future works, we will extended the results to the cases that the controller is not depend on the value of fractional-order.

References

1. Li, C., Peng, G.: Chaos in Chen's system with a fractional order. Chaos Solitons Fractals **22**(2), 443–450 (2004)
2. Hegazi, A., Matouk, A.: Dynamical behaviors and synchronization in the fractional order hyperchaotic Chen system. Appl. Math. Lett. **24**(11), 1938–1944 (2011)
3. Matouk, A.: Stability conditions, hyperchaos and control in a novel fractional order hyperchaotic system. Phys. Lett. A **373**(25), 2166–2173 (2009)
4. Wang, X.-Y., Song, J.-M.: Synchronization of the fractional order hyperchaos Lorenz systems with activation feedback control. Commun. Nonlinear Sci. Numer. Simul. **14**(8), 3351–3357 (2009)
5. Li, C., Liao, X., Yu, J.: Synchronization of fractional order chaotic systems. Phys. Rev. E **68**(6), 067203 (2003)
6. Wu, G.-C., Baleanu, D.: Discrete fractional logistic map and its chaos. Nonlinear Dyn. **75**(1–2), 283–287 (2014)
7. Wu, G.-C., Baleanu, D., Xie, H.-P., Chen, F.-L.: Chaos synchronization of fractional chaotic maps based on the stability condition. Phys. A **460**, 374–383 (2016)
8. Wu, G.-C., Baleanu, D.: Chaos synchronization of the discrete fractional logistic map. Sig. Process. **102**, 96–99 (2014)
9. Muthukumar, P., Balasubramaniam, P., Ratnavelu, K.: Fast projective synchronization of fractional order chaotic and reverse chaotic systems with its application to an affine cipher using date of birth (DOB). Nonlinear Dyn. **80**(4), 1883–1897 (2015)
10. Zhou, P., Bai, R.: The adaptive synchronization of fractional-order chaotic system with fractional-order $1<q<2$ via linear parameter update law. Nonlinear Dyn. **80**(1–2), 753–765 (2015)
11. Maheri, M., Arifin, N.M.: Synchronization of two different fractional-order chaotic systems with unknown parameters using a robust adaptive nonlinear controller. Nonlinear Dyn. **85**(2), 825–838 (2016)
12. Sun, W., Wang, S., Wang, G., Wu, Y.: Lag synchronization via pinning control between two coupled networks. Nonlinear Dyn. **79**(4), 2659–2666 (2015)
13. Padula, F., Alcántara, S., Vilanova, R., Visioli, A.: h_∞ control of fractional linear systems. Automatica **49**(7), 2276–2280 (2013)
14. Fadiga, L., Farges, C., Sabatier, J., Santugini, K.: H_∞ output feedback control of commensurate fractional order systems. In: Proceedings of the European Control Conference, pp. 4538–4543 (2013)
15. Li, J.-N., Zhang, Y., Pan, Y.-J.: Mean-square exponential stability and stabilisation of stochastic singular systems with multiple time-varying delays. Circuits Syst. Signal Process. **34**(4), 1187–1210 (2015)
16. Li, J.-N., Li, L.-S.: Mean-square exponential stability for stochastic discrete-time recurrent neural networks with mixed time delays. Neurocomputing **151**, 790–797 (2015)
17. Li, B., Zhang, X.: Observer-based robust control of $(0<\alpha<1)$ fractional-order linear uncertain control systems. IET Control Theory Appl. **10**(14), 1724–1731 (2016)
18. Ibrir, S., Bettayeb, M.: New sufficient conditions for observer-based control of fractional-order uncertain systems. Automatica **59**, 216–223 (2015)
19. Khamsuwan, P., Kuntanapreeda, S.: A linear matrix inequality approach to output feedback control of fractional-order unified chaotic systems with one control input. J. Comput. Nonlinear Dyn. **11**(5), 051021 (2016)
20. Li, J.-N., Bao, W.-D., Li, S.-B., Wen, C.-L., Li, L.-S.: Exponential synchronization of discrete-time mixed delay neural networks with actuator constraints and stochastic missing data. Neurocomputing **207**, 700–707 (2016)
21. Chen, L., Wu, R., He, Y., Chai, Y.: Adaptive sliding-mode control for fractional-order uncertain linear systems with nonlinear disturbances. Nonlinear Dyn. **80**(1–2), 51–58 (2015)
22. Zhang, R., Yang, S.: Robust synchronization of two different fractional-order chaotic systems with unknown parameters using adaptive sliding mode approach. Nonlinear Dyn. **71**(1–2), 269–278 (2013)
23. Sopasakis, P., Ntouskas, S., Sarimveis, H.: Robust model predictive control for discrete-time fractional-order systems.

In: 23th Mediterranean Conference on Control and Automation (MED), 2015, pp. 384–389. IEEE (2015)
24. Balasubramaniam, P., Muthukumar, P., Ratnavelu, K.: Theoretical and practical applications of fuzzy fractional integral sliding mode control for fractional-order dynamical system. Nonlinear Dyn. **80**(1–2), 249–267 (2015)
25. Li, Y., Li, J.: Stability analysis of fractional order systems based on T–S fuzzy model with the fractional order $\alpha: 0<\alpha<1$. Nonlinear Dyn. **78**(4), 2909–2919 (2014)
26. Boulkroune, A., Bouzeriba, A., Bouden, T.: Fuzzy generalized projective synchronization of incommensurate fractional-order chaotic systems. Neurocomputing **173**, 606–614 (2015)
27. Lin, T.-C., Kuo, C.-H.: H-infinity synchronization of uncertain fractional order chaotic systems: adaptive fuzzy approach. ISA Trans. **50**(4), 548–556 (2011)
28. Pratama, M., Lu, J., Zhang, G.: Evolving type-2 fuzzy classifier. IEEE Trans. Fuzzy Syst. **24**(3), 574–589 (2016)
29. Tavoosi, J., Suratgar, A.A., Menhaj, M.B.: Nonlinear system identification based on a self-organizing type-2 fuzzy RBFN. Eng. Appl. Artif. Intell. **54**, 26–38 (2016)
30. Mohammadzadeh, A., Ghaemi, S.: A modified sliding mode approach for synchronization of fractional-order chaotic/hyperchaotic systems by using new self-structuring hierarchical type-2 fuzzy neural network. Neurocomputing **191**, 200–213 (2016)
31. Doctor, F., Syue, C.-H., Liu, Y.-X., Shieh, J.-S., Iqbal, R.: Type-2 fuzzy sets applied to multivariable self-organizing fuzzy logic controllers for regulating anesthesia. Appl. Soft Comput. **38**, 872–889 (2016)
32. Mendez, G., Juarez, I., Leduc, L., Soto, R., Cavazos, A.: Temperature prediction in hot strip mill bars using a hybrid type-2 fuzzy algorithm. Int. J. Simul. Syst. Sci. Technol. **6**(9), 33–43 (2005)
33. Méndez, G.M., De los Angeles Hernandez, M.: Hybrid learning for interval type-2 fuzzy logic systems based on orthogonal least-squares and back-propagation methods. Inf. Sci. **179**(13), 2146–2157 (2009)
34. MéNdez, G.M., De Los Angeles HernáNdez, M.: Hybrid learning mechanism for interval A2-C1 type-2 nonsingleton type-2 Takagi–Sugeno–Kang fuzzy logic systems. Inf. Sci. **220**, 149–169 (2013)
35. Matignon, D.: Stability results for fractional differential equations with applications to control processing. In: Computational Engineering in Systems Applications, vol. 2, pp. 963–968. Citeseer (1996)
36. Karnik, N.N., Mendel, J.M., Liang, Q.: Type-2 fuzzy logic systems. IEEE Trans. Fuzzy Syst. **7**(6), 643–658 (1999)
37. Sabatier, J., Moze, M., Oustaloup, A.: On fractional systems H_∞-norm computation. In: 44th IEEE Conference on Decision and Control, 2005 and 2005 European Control Conference. CDC-ECC'05, pp. 5758–5763. IEEE (2005)
38. Fadiga, L., Farges, C., Sabatier, J., Moze, M.: On computation of H_∞ norm for commensurate fractional order systems. In: 50th IEEE Conference on Decision and Control and European Control Conference (CDC-ECC), 2011, pp. 8231–8236. IEEE (2011)
39. Li, C., Chen, A., Ye, J.: Numerical approaches to fractional calculus and fractional ordinary differential equation. J. Comput. Phys. **230**(9), 3352–3368 (2011)
40. Li, C., Wang, Y.: Numerical algorithm based on adomian decomposition for fractional differential equations. Comput. Math. Appl. **57**(10), 1672–1681 (2009)
41. Cao, J., Xu, C.: A high order schema for the numerical solution of the fractional ordinary differential equations. J. Comput. Phys. **238**, 154–168 (2013)
42. Yan, Y., Pal, K., Ford, N.J.: Higher order numerical methods for solving fractional differential equations. BIT Numer. Math. **54**(2), 555–584 (2014)
43. Valerio, D.: Toolbox ninteger for Matlab, v. 2.3, September 2005 (2005)
44. Matouk, A., Elsadany, A.: Achieving synchronization between the fractional-order hyperchaotic Novel and Chen systems via a new nonlinear control technique. Appl. Math. Lett. **29**, 30–35 (2014)
45. Aghababa, M.P.: Finite-time chaos control and synchronization of fractional-order nonautonomous chaotic (hyperchaotic) systems using fractional nonsingular terminal sliding mode technique. Nonlinear Dyn. **69**(1–2), 247–261 (2012)
46. Xu, B.: Chaotic synchronization of nonlinear-coupled fractional-order Liu system and secure communication. In: 2015 International Symposium on Computers and Informatics. Atlantis Press (2015)
47. Zhen, W., Xia, H., Ning, L., Xiao-Na, S.: Image encryption based on a delayed fractional-order chaotic logistic system. Chin. Phys. B **21**(5), 050506 (2012)
48. Wu, G.-C., Baleanu, D., Lin, Z.-X.: Image encryption technique based on fractional chaotic time series. J. Vib. Control **22**(8), 2092–2099 (2016)